Growth, crystal structure, spectral, optical and theoretical studies on L-Alanine oxalate crystals

[1]K. Deepa, [2]S. Senthil, [1]J. Madhavan [*]
[1]Research Scholar, [2]Assistant Professor, [3]Associate Professor
[1]Department of Physics, Loyola College, Chennai, India
[2]Department of Physics, Government Arts College for Men, Nandanam, Chennai, India
[3]Department of Physics, Loyola College, Chennai, India

Abstract **- Transparent optical quality single crystals of L-alanine oxalate (LAO) were grown by slow solvent evaporation technique. Crystal structure of the as-grown L-alanine oxalate (LAO) was determined by single crystal X-ray diffraction analysis. The powder X-ray diffraction study reveals the crystallinity of the as-grown crystal and it is compared with that of the experimental one. The functional groups are identified by Fourier transform infrared spectral analysis and compared with theoretical spectrum. The crystal is stable up to the melting point and the mechanistic behavior is ascertained by microhardness studies. Second harmonic generation (SHG) activity of L-alanine oxalate (LAO) is significant as estimated by Kurtz and Perry powder technique. HOMO–LUMO energies and first order molecular hyper polarizability of L-alanine oxalate (LAO) have been evaluated using density functional theory (DFT) employing B3LYP functional and 6-31G (d,p) basis set. Optical absorption behavior of the grown crystal was examined by recording the optical spectrum and band gap energy was also estimated.**

Key words **- Single crystal XRD, FTIR, DFT, Microhardness**

I. INTRODUCTION

Second-order nonlinear optical (NLO) materials are of crucial importance for applications in telecommunication technology and quantum electronics. The current research on organic materials is due to their exceptionally large second-order nonlinearity and the virtually unlimited variety of crystal structures. Compared to their inorganic compounds, organic NLO materials have advantages such as large NLO coefficients and structural diversity. But organic NLO materials have some intrinsic weaknesses such as poor physico–chemical stability and low mechanical strength. Hyperpolarizability is the one of the important nonlinear optical property. Higher the hyperpolarizability, greater will be the charge transfer. We have reported some organic crystals with high first order molecular hyperpolarizability but with small second harmonic generation (SHG) efficiency [1–3]. In this chapter, we will report on synthesis, growth, structure and properties of L-alanine oxalate (LAO). The detailed vibrational spectral studies are aided by DFT calculations to elucidate the assignment of the vibrational spectra and the highest occupied molecular orbital (HOMO), lower unoccupied molecular orbital (LUMO) and the first order hyperpolarizability of this compound is examined. Optical parameters are analyzed with incident photon energy from experimentally obtained UV absorption data and theoretical equations. Hardness, dielectric, SHG efficiency and Photoconductivity nature of the material are also studied.

II. EXPERIMENTAL PROCEDURES

Equimolar amounts of L-alanine and oxalic acid were dissolved in double distilled water to prepare the aqueous solution of LAO. In deionized water, L-alanine and oxalic acid are allowed to react by the following chemical reaction to produce

$CH_3CHNH_3COOH + H_2C_2O_4 \rightarrow C_5H_9NO_6$

The synthesized salt of LAO was obtained by evaporating the solvent. The synthesized salt was used to measure the solubility of LAO in water **Fig.1**. The supersaturated solution was prepared in accordance with the solubility data. Single crystals of LAO were grown from aqueous solution using slow solvent evaporation technique. The solvent was allowed to evaporate and numerous tiny crystals were formed at the bottom of the container due to spontaneous nucleation. The transparent and defect free ones among them were chosen as the seeds for growing bulk crystals. Good optical quality crystals of dimension up to 19x3x6 mm^3 were harvested after a period of 20−30 days. The photographs of as grown crystals of LAO are shown in **Fig .2.**

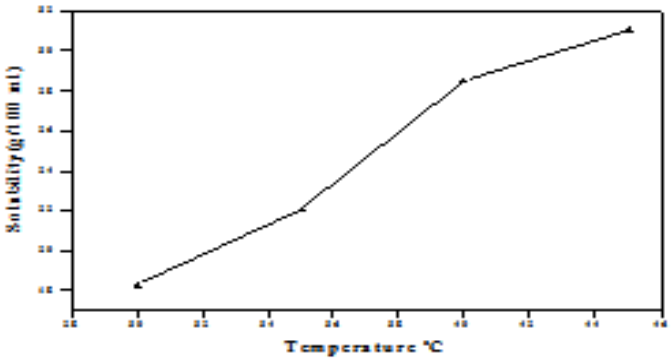

Figure.1. solubility diagram of LAO

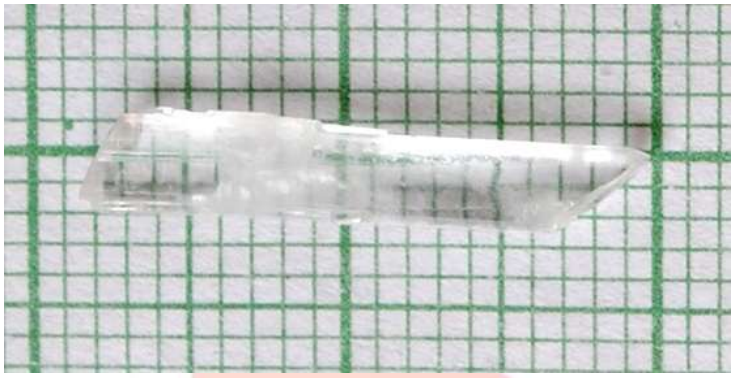

Figure.2. Photograph of as grown LAO single crystal

III. RESULTS AND DISCUSSION

Single crystal XRD

The structural analysis of LAO crystal was carried out by single crystal XRD analysis and the crystallographic parameters are listed in Table 1. It belongs to orthorhombic crystal system having non-Centro symmetry with $P2_12_12_1$ space group. Lattice parameters have been determined as a=5.6034(5) Å, b=7.2353(6) Å, c=19.597(3) Å, $\alpha=\beta=\gamma=90^{\circ}$ and the volume of the unit cells is found to be 798.3 (2) $Å^3$. Theoretically simulated XRD pattern and experimentally obtained Powder XRD pattern are shown in **Fig.3** and **Fig.4** respectively.

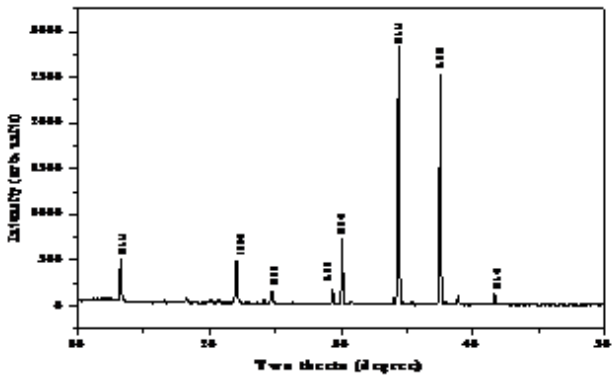

Figure.3 Experimentally obtained Powder XRD pattern of LAO

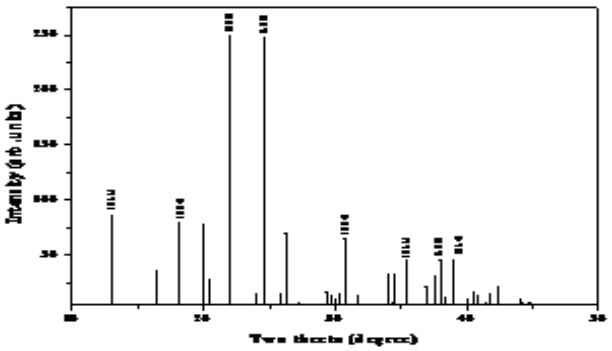

Figure .4 Theoretically simulated powder XRD pattern of LAO

Table-1 Crystal parameters of LAO

Empirical Formula	$C_5H_9NO_6$
Formula Weight	179.13
Temperature	293(2)K
Wavelength	1.54180A˚
Crystal System	Orthorhombic
Space Group	P $2_12_12_1$
Unit cell Dimensions	a = 5.6304(5) A˚ b = 7.2353(6)A˚ c = 19.597(3) A˚ $\alpha = \beta = \gamma = 90^{\circ}$
Volume	798.3(2) A°^{3}
Z	4
Calculated Density	1.490 g/cm^3
Absorption co- efficient	1.229mm^{-1}
F(0 0 0)	376
Crystal size	0.2 x 0.15 x 0.11 mm^3
Theta range of data Collection	4.51 – 67.91˚
Reflections collected	879
Independent reflections	853
Refinement method	Full matrix least squares on F^2
Data/restraints/parameters	853/0/112
Goodness – of – fit on F^2	1.092
Final R indices [l>2σ(l)]	R_1 = 0.0304 wR_2 = 0.0826
R indices (all data)	R_1 =0.0312 wR_2 = 0.0884

Computational details

A density functional theory investigation for minimum energy state of LAO molecule is carried out.

Geometrical structure

The numbering system adopted for LAO in this investigation is shown in **Fig.5.** As there are two rotamers, viz., the Oxalic and the amino moieties, the molecule can exist in a variety of conformations. A B3LYP/6-31G(d,p) level on full geometry optimization with different spatial dispositions following the standard geometrical parameters, the converged final geometry was the one with all heavy atoms in a plane, with both the hydrogen atoms of the amino group and two of the hydrogen atoms of the methyl group lying out-of-plane. The relevant geometrical parameters like bond length and bond angles have been collected in Tables 2 and 3. It is found from the tables that minimum energy bond length and bond angles are compared with Single crystal

XRD parameters. Bond lengths obtained from XRD analysis are smaller than Gaussian values. The differences between this can be attributed to the fact that the theoretical calculations were carried out with isolated molecules in the gaseous phase but the experimental values were based on molecules in the crystalline state [4].

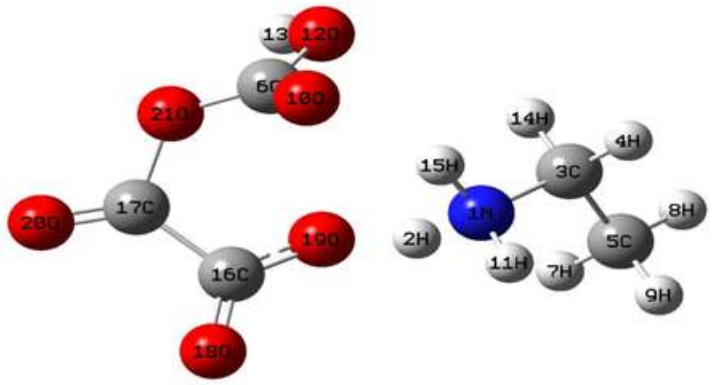

Figure .5 Atomic numbering systems adapted for ab initio computations of LAO molecule.

Table 2 Selected bond length of LAO molecule

S.No	Bondlength(A˚)	XRD	Gaussian
1	N_1- H_{15}	0.8900	1.03314
2.	N_1– H_{11}	0.8900	1.02123
3.	N_1– C_3	1.483(3)	1.50996
4.	C_3- H_{14}	0.9600	1.09283
5.	C_3– H_4	0.9600	1.09436
6.	C_3 – C_5	1.522(3)	1.52647
7.	C_5 – H_8	0.9600	1.09442
8.	C_5 – H_9	0.9800	1.09667
9.	C_5 – H_7	0.9800	1.09471
10	C_6 – O_{12}	1.199(2)	1.36148
11.	C_6 – O_{10}	1.219(2)	1.23060
12	C_6 – O_{21}	1.297(2)	1.38068
13.	O_{12} – H_{13}	0.8200	0.97978
14.	C_{17} – O_{21}	1.303(2)	1.46055
15.	C_{17} – O_{20}	1.205(2)	1.20749
16.	C_{17} – C_{16}	1.548(3)	1.54770
17.	C_{16} – O_{18}	1.235(2)	1.24278
18.	C_{16} – O_{19}	1.303(2)	1.30980

Table 3 Selected bond angles of LAO molecule.

Bond Angle(degree)	XRD	GAUSSIAN	Bond Angle(degree)	XRD	GAUSSIAN
H_{15}-N_1-H_{11}	109.5	110.79229	C_{17}-C_{16}-O_{19}	111.32	112.73023
H_{15}-N_1-C_3	109.5	111.47857	O_{20}-C_{17}-O_{21}	126.65(19)	117.81369
H_{11}-N_1-C_3	109.5	112.40390	C_{17}-O_{21}-C_6	120.5	121.77214
H_{14}-C_3-H_4	109.5	108.37728	O_{21}-C_6-O_{12}	109.5	111.57625
H_4-C_3-C_5	109.6	111.88045	O_{21}-C_6-O_{10}	125.65(18)	125.93896
H_7-C_5-H_8	109.5	108.24001	O_{12}-C_6-O_{10}	126.65	122.09844
O_{18}-C_{16}-O_{19}	126.7	129.51111	H_{13}-O_{12}-C_6	109.5	111.36942

C_{17}-C_{16}-O_{18}	118.05	117.75787	O_{10}-C_6-O_{12}	121.6	120.
C_3-C_5-H_8	109.5	109.5	H_{14}-C_3-C_5	109.65	111.46980

Hyperpolarizability studies

Interests in organic optoelectronic materials and devices have motivated experimental and theoretical studies of molecular structures with enhanced hyperpolarizabilities. [5]Molecules with electronic asymmetry, or "push-pull" donor- bridge-acceptor electronic framework, have been demonstrated to have large first hyperpolarizabilities (β) [6] Interests in organic optoelectronic materials and devices have motivated experimental and theoretical studies of molecular structures with enhanced hyperpolarizabilities. Molecules with electronic asymmetry, or "push-pull" donor- bridge-acceptor electronic framework, have been demonstrated to have large first hyperpolarizabilities (β). The first static hyperpolarizability (β_0) and its related properties (β α_0 and Δα) have been calculated using B3LYP/6-31G level based on finite field approach. The components of β are defined as the coefficients in the Taylor series expansion of the energy in the external electric field.

Table 4 Hyperpolarizability of LAO in esu

β_{xxx}	123.6388637
β_{xyy}	35.2443193
β_{xzz}	42.7272488
β_{yyy}	-3.1986838
β_{yzz}	3.6918875
β_{yxx}	-138.9561625
β_{zzz}	22.4016694
β_{zxx}	-5.5371442
β_{xyy}	38.7531654
$\beta_{tot(esu)}$	$2.09921105x10^{-30}$

To calculate the hyperpolarizability, the origin of the Cartesian coordinate system was chosen as the center of mass of the compound [7]. The calculated first hyperpolarizability of LAO is 2.84×10^{-30} esu which is 2 times that of KDP. The calculated first hyperpolarizability components are given in Table 4.

HOMO-LOMO Analysis:

Both the highest occupied molecular orbital (HOMO) and the lowest unoccupied molecular orbital (LUMO) are the main orbital take part in chemical stability. The HOMO represents the ability to donate an electron, LUMO as an electron acceptor represents the ability to obtain an electron. The HOMO and LUMO energy calculated by B3LYP/6-31G(d,p) method as shown below:

HOMO energy (B3LYP) = -0.25105a.u

LUMO energy (B3LYP) = -0.06410a.u

HOMO–LUMO energy gap (B3LYP) = -0.18695a.u

The HOMO is located over the phenyl ring and the carboxylic acid group attached to the phenyl ring. The HOMO →LUMO transition implies an electron density transfer to the carboxylic acid group from the phenyl ring. Moreover, these orbital significantly overlap in their position for LAO **Fig.6.** The HOMO and LUMO energy gap explains the eventual charge transfer interactions taking place within the molecule.

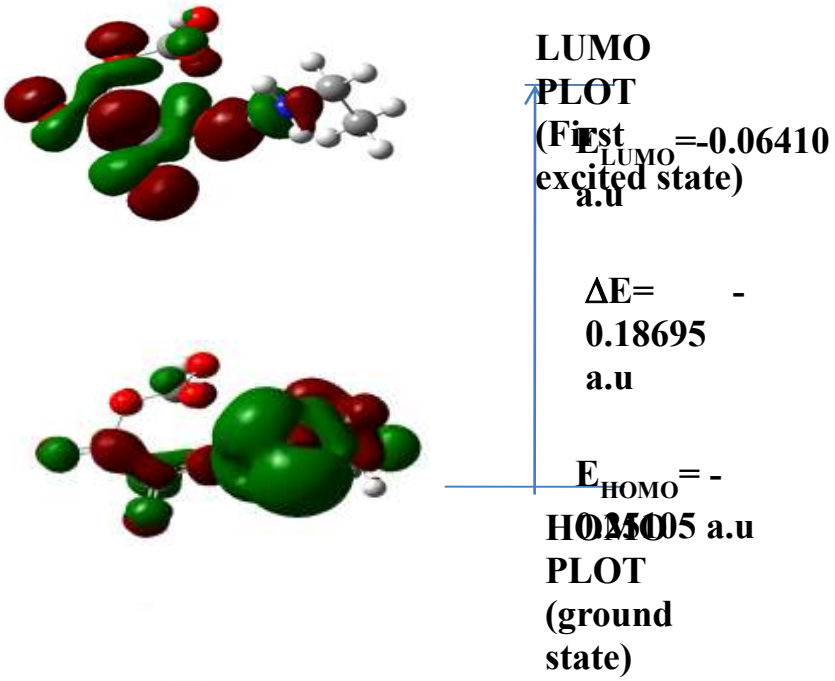

Figure 6 HOMO – LUMO plot of LAO molecule.

Vibrational Analysis

The LAO molecule has 21 atoms, which possess 57 normal modes of vibrations. All vibrations are active in infrared spectrum. The normal modes of LAM are distributed amongst the symmetry species as 39 in plane and 18 out plane vibrations. Usually the calculated harmonic vibrational wave numbers are higher than the experimental ones, because of the anharmonicity of the incomplete treatment of electron correlation and of the use of finite one-particle basis set. The harmonic frequencies were calculated by B3LYP method using 6-31G (d, p), basis sets experimentally observed and theoretically calculated harmonic vibrational frequencies and their correlations were gathered in Table 5. From the calculations, the computed values are in good agreement with the observed values. The FT-IR spectrum of LAO was recorded using BRUKER IFS-66V spectrometer in the range between 4000 and 500cm^{-1}. The resulting spectrum is shown in **Fig .7.** It coincides well with theoretically simulated FT-IR spectrum shown in Figure.8. Force constant, reduced mass and theoretically simulated IR intensity of the LAO molecule are given in Table 5.

NH_3 Vibrations

The zwitterionic form molecules, the NH_3 asymmetric and symmetric stretching bands, normally appear in the region 3330 and 3080 cm^{-1}, respectively [8]. The strong band observed in IR vibrations at 3054 cm^{-1} corresponds to NH_3 asymmetric stretching mode. It has experimental counterpart at 3030 cm^{-1}. The red shifting of NH_3 stretching wave numbers indicate the formation of intramolecular N–H···O hydrogen Bonding. The short H . . . O distance (H13. . .O12 = 0.9797A˚) also supports the existence of N–H···O hydrogen bonding. The NH_3 asymmetric deformation vibrations usually appear in the region 1660–1610 cm^{-1} and that of the symmetric deformation in the region 1550–1485 cm^{-1} **[9]**. In LAO, the NH_3 asymmetric deformation vibrations are observed as a very strong band at 1557 cm^{-1} in IR and the symmetric bending modes are observed as a strong band in IR at 1537 cm^{-1}.Both the vibrations has its experimental values at1560 and1513 cm^{-1}. The NH_3 rocking modes appear as a weak band in IR at 962 cm^{-1} and torsions at 39 cm^{-1}.

Carbonyl vibrations

The C=O stretching vibrations give raise to the characteristic band in IR spectrum, and the intensity of these band can increase owing to the conjugation or formation of hydrogen bonds. The carbonyl stretching vibrations are expected in the region 1760–1730 cm^{-1} **[10]**. In LAO, there are three carbonyl groups (C6= O10, C16 =O18 and C17= O31). The very strong IR band at 1731 cm^{-1} correspond to C= O stretching modes and coincides with the experimental spectrum at 1724 cm^{-1}. When a carbonyl group participates in hydrogen bonding, resonance can occur, which puts a partial negative charge on the oxygen atom accepting the hydrogen bond and a positive charge on the atom donating the hydrogen, the partial 'transfer of allegiance' of the proton enhances resonance and lowers the C= O stretching wave number. The lowering of carbonyl stretching mode is attributed to the fact that the carbonyl group chelate with the other nucleophilic groups, thereby forming both intra and intermolecular hydrogen bonding in the crystal.

Hydroxyl vibrations

The OH stretching vibrations are sensitive to hydrogen bonding. The non-hydrogen-bonded or free hydroxyl group absorbs strongly in the 3600–3550 cm^{-1} region, whereas the existence of intermolecular hydrogen bond formation can lower O–H stretching wave number around 3500 cm^{-1} with increase in IR intensity **[10]**. This theory holds well in the present study. The strong bands observed

in IR at 3331 and 3146 cm^{-1} correspond to OH stretching vibrations. The red shifting of OH stretching wave numbers are giving clear evidence for the intermolecular O–H· · ·O hydrogen bonding in the molecule. The in-plane bending of O–H group usually appears as strong bands in the region 1440–1260 cm^{-1} **[9]**. The strong bands at 1261 and 1076 cm^{-1} in the IR spectrum are assigned to OH in plane bending mode. The O–H out of plane bending vibration gives rise to a strong band in the region 700–600 cm^{-1} **[10]**. The calculated values of OH group vibrations are in good agreement with the experimental results.

Table 5 Vibrational Assignments of LAO Molecule

Frequency	Experimental frequency (cm^{-1})	Spectroscpic assignment	IR intensity (KM/Mole)	Force constant (mDyne/A°)	Reduced mass(amu)
3641.0169	-	NH st	71.9725	8.3194	1.0651
3525.2361	-	NH_2 asy st	49.3563	7.9127	1.0807
3331.6631	3341	OH st	177.1868	6.9319	1.0599
3158.8209	-	O-H st	14.8743	1.1057	1.1057
3146.7113	3135	C-H st	10.6923	6.4137	1.0994
3124.3879	-	CH_2 ips	10.0839	6.3190	1.0987
3090.9085	-	C-H st	13.8345	5.9790	1.0622
3054.0305	3030	NH_3asy st	13.5063	5.6998	1.0372
1828.7112	1814	C =O st	132.2124	23.9472	12.1539
1779.6634	-	C-C st	59.3880	4.3220	2.3161
1731.3753	1724	C =O st	403.0538	4.2672	2.4161
1727.1042	-	C=C st	255.0179	2.1343	1.2144
1688.1727	1692	C =N st	270.9033	2.1379	1.2732
1644.7270	1630	CH_2 ipb	865.4607	2.7875	1.7490
1557.4007	1560	NH_3 asy def	21.3002	1.5527	1.0865
1544.6808	1538	C=C st	15.2743	1.4739	1.0484
1537.6173	1513	NH_3 sy b	6.3549	1.4493	1.0404
1470.1417	1483	CH ipb	16.9270	1.5320	1.2031
1439.6680	1440	CH_2 sci	64.7713	1.6001	1.3103
1373.3448	1389	CH opb	13.5104	1.2841	1.1555
1293.6977	1309	CH_2 wag	877.1389	5.8857	5.9687
1287.6724	-	NH_3 tw	20.9560	1.4732	1.5080
1261.8902	-	OH ipb	45.4225	1.4083	1.5010
1255.8987	-	C-N st	158.1905	1.9490	2.0973
1191.6827	1146	CH_2 roc	29.4623	2.3333	2.7887
1076.3151	1102	OH ipb	29.5365	1.0936	1.6023
1060.6128	1069	PhI	24.6696	0.9601	1.4486
1020.8551	-	NH_2 t	15.5445	0.9602	1.5637
966.1956	991	R asyd	283.2435	6.2753	11.4091
962.8158	965	NH_3 roc	78.3274	7.2954	13.3571
880.0578	855	CC	3.6153	1.3124	2.8761
835.2978	819	CH opb	23.0544	0.4539	1.1042
794.7566	-	R opb	42.3301	4.3985	11.8190
784.3327	773	R berth	129.7208	4.1534	11.4592
686.8864	658	O-H opb	43.1214	3.4271	12.3284
670.7739	-	NH b	5.3482	2.7267	10.2858
600.6463	605	CN ipd	25.3086	1.9742	9.2878
586.6138	580	C-CO b	27.0439	2.1301	10.5061
548.2281	536	C-C b	135.7866	0.2126	1.2008
514.6009	522	COO^- roc	14.6141	0.2030	1.3011
468.8169	-	C-C b	107.1803	0.7797	6.0207
418.8364	-	C-C opb	20.5300	0.5787	5.5994

396.8678	-	R opb	3.1277	0.1898	2.0454
386.4879	-	C-C b	11.8996	0.6776	7.6994
355.1889	-	C-H	39.9763	0.4686	6.3036
294.3132	-	N-H st	17.3481	0.3921	7.6828
247.9294	-	NH_2 t	2.6787	0.0476	1.3145
204.8696	-	CO opb	5.7160	0.1551	6.2715
166.1278	-	C-C	21.7482	0.0793	4.8777
128.3344	-	C-C-N ipb	8.5613	0.0254	2.6186
100.6144	-	CC ipb	2.0537	0.0398	6.6733
89.6354	-	R tor	8.9999	0.0250	5.2862
63.3078	-	CNH_2 t	6.1209	0.0088	3.7280
47.9839	-	R tor	0.4398	0.0051	3.7536
39.9448	-	NH_3 tor	2.0039	0.0076	8.0795
31.7170	-	CC ben	0.0499	0.0026	4.3108

St-stretching ; **sym st**- symmetry stretching ;**asy st**- assymtry stretching ; **sci**-scisorring **t**-twisting ; **tor**-torsion ;**ipb**-in-planebending ; **opb**- out-of-plane bending; **ipd**-inplane deformation **wag**- wagging; **R**-anthracene ring;; **roc**-rocking;

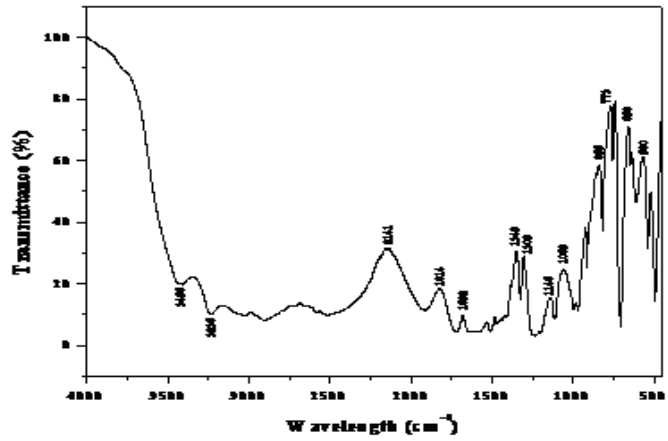

Figure 7 Experimentally obtained FTIR spectrum of LAO

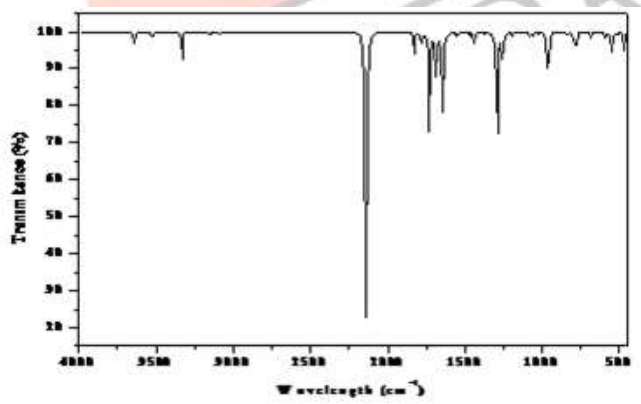

Figure 8 theoretically simulated FTIR spectrum of LAO

Optical Properties of LAO

UV–vis spectrum of LAO has been recorded in the wavelengthrangeof200–1200nm by using Perkin Elmer Lamda 35 UV–vis spectro photo meter at room temperature and is shown in , **Fig.9** was obtained with a crystal of thickness 2 mm. The absorption spectrum plays a vital role in identifying the potential of a NLO material because a given NLO material can be of utility only if it has a wide transparency window without any absorption at the fundamental and second harmonic wavelengths and preferably with the lower limit of the transparency window being well below the 300 nm limits. From the graph, it is evident that the crystal has a transparency window from 230 nm onwards suggesting the suitability of LAO for SHG of the 1064nm radiation and for other applications in the blue-violet region.

There is no appreciable absorption of light throughout the visible range, as is the case of all the amino acids. The optical losses in the higher wavelength side could also be reduced by optimizing the growth conditions towards the production of crystals

of higher quality. The values of the optical band gap E_g were obtained from the intercept of $(\alpha h\nu)^2$ versus $h\nu$ curve plotted. The Band gap of LAO is found as 3.9 eV and other linear optical parameters such as extinction coefficient, reflectance, refractive index, complex dielectric constant and optical conductivity are calculated. It's found that the candidate material has low extinction co efficient, low refractive index and high optical conductivity. These suitable values makes the material highly NLO active. **Fig .9 to 15.** Explain the variation of linear optical constants with incident photon energy for LAO single crystal.

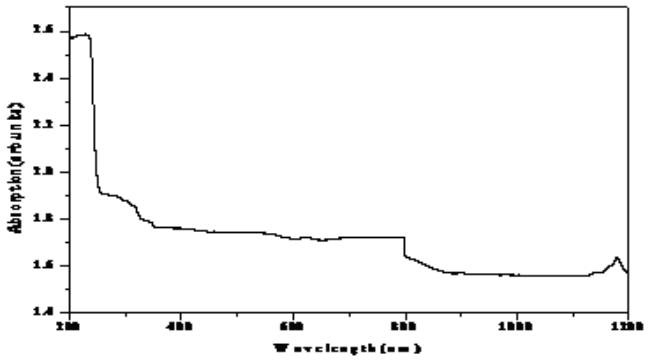

Figure 9 Optical absorption spectrum of LAO

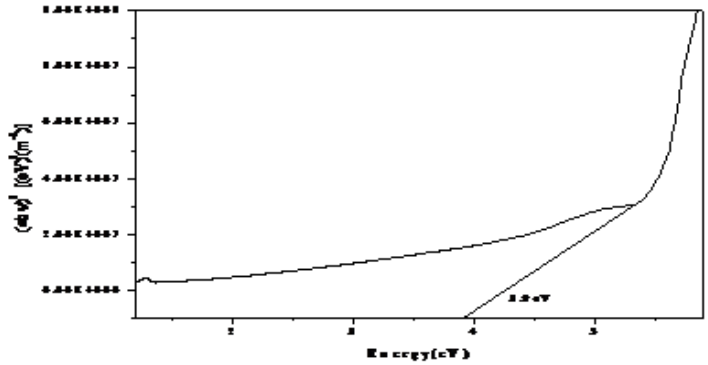

Figure 10 Energy band gap of LAO

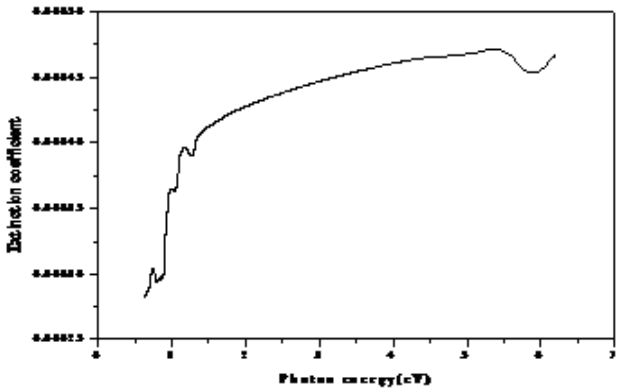

Figure 11 Extinction coefficient Vs Incident Photon Energy of LAO

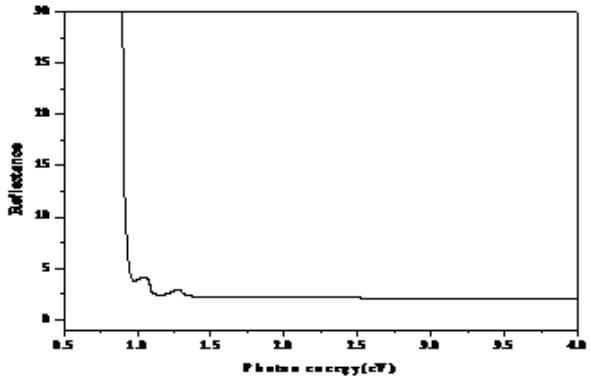

Figure 12 Reflectance Vs Incident photon energy of LAO

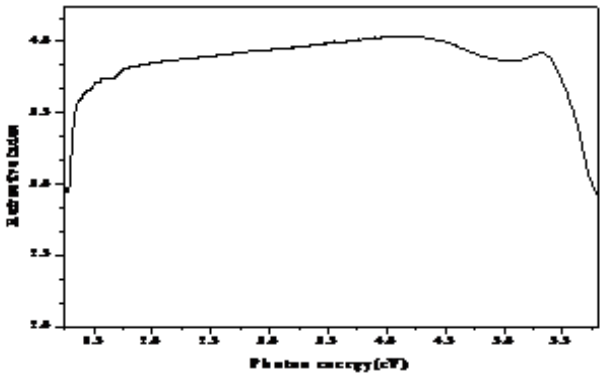

Figure 13 Refractive index Vs Incidient photon energy of LAO

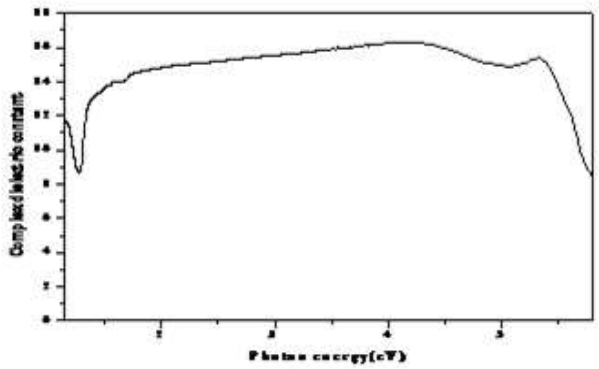

Figure 14 Complex dielectric constant Vs Incident photon energy of LAO

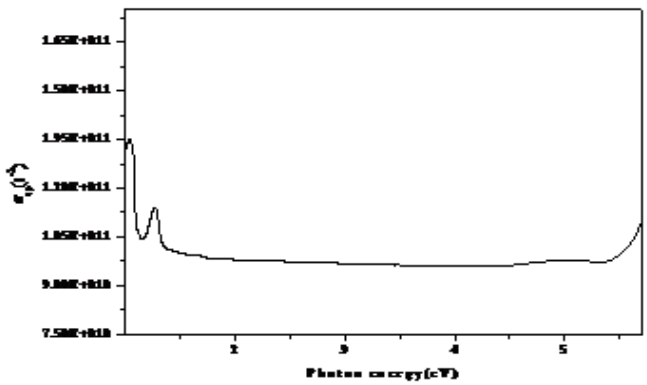

Figure 15 Optical conductivity Vs Incident photon energy of LAO

Microhardness studies

Vickers hardness test was carried out on a polished sample of LAO using SHIMADZU HMV microhardness tester at room temperature. Several indentations were made for each load at a constant indentation time of 10 s and the Vickers hardness number (Hv) was evaluated for the loads varying from 10 to 50 g. The plot **Fig.16** drawn between the Hv and the applied load indicates that the Hv decreases with increasing load, which is normally attributed to the normal indentation size effect (ISE). In order to know the hardness nature of the material, the work hardening coefficient (n) was determined from the plot between log *p* and log *d* **Fig.17** by the least square fit method. The value of 'n' is found to be 1.73, thus indicating the soft nature of LAO.

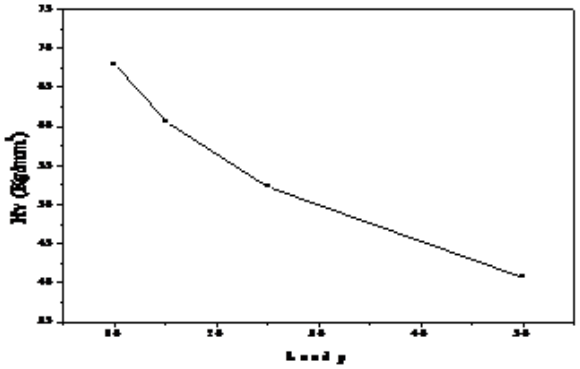

Figure 16 Vickers hardness number Vs applied load of LAO

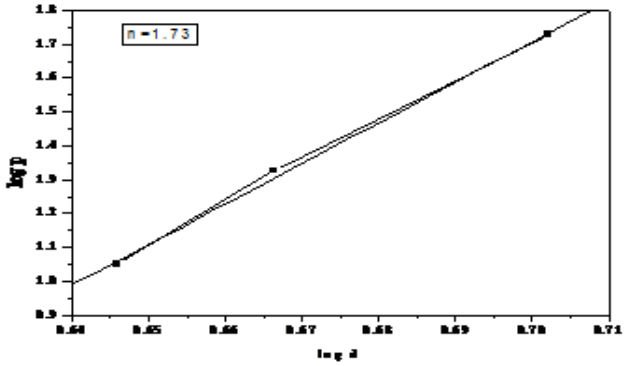

Figure 17 log P Vs log d of LAO

NLO studies

The SHG measuring set up consists of a Q switched Nd:YAG laser of 1064 nm whose beam falls on to a thin section of the material. The second harmonic green light at 532 nm is finally detected using an optical cable attached to a fluorescence spectroscope. For the SHG efficiency measurements, microcrystalline material of KDP was used for comparison. When a laser input of 6.2 mJ was passed through LAO, second harmonic signal of 122 mW is produced and the experimental data confirm a second harmonic efficiency of nearly 1 times that of KDP (124 mW).

Conclusions

Single crystal of L-alanine Oxalate has been grown successfully by slow evaporation growth technique at room temperature. Single crystal XRD studies were carried out for the grown crystal. The single crystal analysis shows that the crystal belongs to orthorhombic crystal system with $P2_12_12_1$ space group. The powder X-ray diffraction study reveals the structure and crystallinity of the grown crystal land simulated pattern coincides with experimental one with varied intensity patterns. (DFT) computations of LAO molecule calculated by DFT (BLYP) level with 6-31G (d,p) basis set gives the optimized structure. Experimentally obtained bond lengths and bond angles are compared with theoretically calculated one. The optical properties of the grown crystal were evaluated from the absorption spectrum. Various linear optical parameters are calculated and analyzed as a function of incident photon energy. Theoretical and experimental IR spectroscopic analysis was carried out and the presence of functional groups in LAO molecule was qualitatively analyzed. HOMO-LUMO analysis reveals the molecular energy gap. The second harmonic generation of the grown crystal was measured and compared with KDP. From micro hardness test, it is observed that hardness number H_v decreases with the increase in load and the work hardening coefficient n was calculated as 1.73.

REFERENCES

[1] J. Madhavan, S. Aruna, K. Prabha, J. Packium Julius Ginson, P. Joseph, S. Selvakumar, and P. Sagayaraj, "Growth and characterization of a novel NLO crystal L-histidine hydrofluoride dihydrate (LHHF)", Journal of Crystal Growth, vol. 293, pp.409–414,2006.

[2] M. Rajasekar, K. Muthu, A. Aditya Prasad, S.P. Meenakshisundaram "Growth, hyperpolarizability, characterization and theoretical studies of NLO active tris(allylthiourea)mercury(II) chloride", Journal of Molecular Structure , vol. 1085, pp. 147–154, 2015.
[3] K. Sangeetha , L.GuruPrasad , R.Mathammal, "Crystal growth, vibrational, optical, thermal and theoretical studies of a nonlinear optical material: 2-Methyl 3,5-dinitrobenzoic acid", PhysicaB, vol.501,pp. 5–17, 2016.
[4] J. Madhavan, S. Aruna, P. C. Thomas, M. Vimalan, S. A. Rajasekar, and P. Sagayaraj, "Growth and characterization of L-histidine hydrochloride monohydrate single crystals", Cryst. Res. Technol. vol. 1,pp. 59-64, 2007.
[5] D.A.B. Miller, and D.S. Chemla, "Theory of the linear and nonlinear optical properties of semiconductor microcrystallites", vol.35, pp. 8113-8125, May 1987.
[6] K. Victor Chow, and Karen C. Denning, "A simple multiple variance ratio test", Journal of Econometrics, vol. 58, pp385-401,1993.
[7] C.Adant, M .Durpuis , JL Bredas, "Ab initio study of the nonlinear optical properties of urea: Electron correlation and dispersion effects", Int.J.Quantum Chem.,Vol.56,pp 497-507, 2004.
[8] D. S. Chemla and J. Zyss, "NonlinearOptical Properties of Organic Molecule and Crystals," Academic press, New York, 1987.

[9] R. M. Silverstein, G. Clayton Bassler and T. C. Morrill, "Spectroscopic Identification of Organic Compounds," 4th edition, John Wiley & Sons, New York, 1981.
[10]. N.B. Colthup, L.H. Daly, S.E. Wiberley, "Introduction to Infrared and Raman Spectroscopy", Ed 3, Academic Press, New York, pp.301-305, 1990.